PHYSICAL REVIEW D **80,** 114021 (2009)

Phase space and jet definitions in soft-collinear effective theory

William Man-Yin Cheung,* Michael Luke,† and Saba Zuberi‡

Department of Physics, University of Toronto, 60 St. George Street, Toronto, Ontario, Canada M5S 1A7

(Received 20 October 2009; published 21 December 2009)

We discuss consistent power counting for integrating soft and collinear degrees of freedom over arbitrary regions of phase space in the soft-collinear effective theory, and illustrate our results at one-loop with several jet algorithms: JADE, Sterman-Weinberg and $k_\perp$. Consistently applying soft-collinear effective theory power counting in phase space, along with nontrivial zero-bin subtractions, prevents double counting of final states. The resulting phase space integrals over soft and collinear regions are individually ultraviolet divergent, but the phase space ultraviolet divergences cancel in the sum. Whether the soft and collinear contributions are individually infrared safe depends on the jet definition. We show that while this is true at one-loop for JADE and Sterman-Weinberg, the $k_\perp$ algorithm does not factorize into individually infrared safe soft and collinear pieces in dimensional regularization. We point out that this statement depends on the ultraviolet regulator, and that in a cutoff scheme the soft functions are infrared safe.

DOI: 10.1103/PhysRevD.80.114021 PACS numbers: 12.38.Bx, 12.39.St, 13.87.−a, 13.87.Ce

I. INTRODUCTION

The study of jets provides an important tool to investigate strong interactions and tests QCD over a wide range of scales, from partonic hard scattering to the evolution of hadronic final states that make up the jets. Hadronic jets also play an integral role in searches for physics beyond the standard model. Soft-collinear effective theory (SCET) [1–5] provides a useful framework to study jets, reproducing results from QCD obtained from traditional factorization techniques (see, for example, [6,7]) while systematically including power corrections and organizing perturbative resummation.

The effective theory separates the scales of the underlying hard interaction from the scales associated with the collinear particles in the jets and the long-distance soft physics. Unlike QCD, particles in SCET whose momenta have parametrically different scaling are described by separate fields—in this case, either (ultra-)soft or collinear.[1] Their light-cone components, $p = (n\cdot p, \bar{n}\cdot p, p_\perp) = (p^+, p^-, p^\perp)$ scale as

$$p_s \sim Q(\lambda^2, \lambda^2, \lambda^2), \qquad p_c \sim Q(1, \lambda^2, \lambda) \tag{1}$$

where n and $\bar{n}$ are light-cone vectors in the $\pm\vec{n}$ direction and λ is a small dimensionless parameter which is determined by the dynamics. At leading order in λ the soft and collinear modes decouple in the SCET Lagrangian. These properties of the effective theory have been utilized to prove factorization, resum large logarithms, and parametrize nonperturbative corrections for event shapes in the two-jet limit [8–11] and for massive top quark jets [12], for example. The factorization of generic fully differential jet cross sections has also been shown independent of jet observables for e^+e^- and pp collisions [13]. For an n-jet cross section with a given jet definition to fully factorize, however, the phase space constraints should also factorize appropriately in the effective field theory (EFT). Such factorization of phase space constraints has not yet been shown in any scheme other than the hemisphere scheme [13] (in which all events are dijet).

In this paper we study the two-jet cross section for e^+e^- collisions in SCET, using three jet algorithms: a cone algorithm, Sterman-Weinberg (SW) [14], which defines a jet based on an angular cut and was considered in the context of SCET in [8,9,15], as well as two clustering algorithms, JADE [16] and $k_\perp$ [17], which iteratively combine partons into jets based on kinematic conditions. This is a first step towards the broader goal of determining the appropriate factorization theorem and resumming logarithms using SCET. While we do not consider here the more general problem of factorization theorems for jets, we point out some implications of our results for factorization theorems, in particular, showing that the form of the factorization in SCET depends on the ultraviolet regulator. The main point of this paper is instead to demonstrate the relationship between the cutoffs in the effective field theory and phase space limits, and to consider their implications for dijet rates in SCET. Since SCET has no hard cutoff separating soft from collinear regions of phase space, some care is required to perform phase space integrals consistently. The next-to-leading-order (NLO) dijet rate in SCET also demonstrates the interplay of divergen-

*mycheung@physics.utoronto.ca
†luke@physics.utoronto.ca
‡szuberi@physics.utoronto.ca

[1]In situations with multiple collinear directions, there are collinear modes for each direction.

ces between the soft and collinear sectors, and provides nontrivial examples of the zero-bin subtraction [18].

II. PHASE SPACE IN QCD AND SCET

At each order in perturbation theory, a jet algorithm corresponds to a scheme to partition the available phase space into regions with different numbers of jets. At $O(\alpha_s)$, the phase space for $e^+e^- \to$ hadrons or hadronic Z decay was discussed in SCET in [18] using the variables $x_i = \frac{2p_i\cdot q}{q^2}$, where $q = p_1 + p_2 + p_3$ is the total momentum of the process and $p_{1,2,3}$ are the momenta of the quark, antiquark, and gluon, respectively. In our discussion we will find it more convenient to choose the independent variables to be the light-cone components of the gluon momentum, $p_3^+ \equiv n\cdot p_3$ and $p_3^- \equiv \bar{n}\cdot p_3$, and fix the coordinates by choosing the antiquark to be moving purely in the $\bar{n}$ direction (i.e. $p_2^- = p_2^\perp = 0$). The resulting phase space is illustrated schematically in Fig. 1. Note that because our choice of coordinates is not symmetric in the n and $\bar{n}$ directions, the phase space is not symmetric under exchange of the p_3^+ and p_3^- axes. (For example, in the upper left the antiquark is constrained to be soft, while in the lower right the quark and antiquark recoil against the gluon, and so either the quark or the antiquark may be soft, or both may be $\bar{n}$-collinear.)

In the shaded regions, two of the partons recoil approximately back-to-back and the third is either soft or recoils roughly parallel with one of the other two, while in the central unshaded region all three partons recoil in different directions. Thus, the shaded region roughly corresponds to two-jet events, while the central region corresponds to three-jet events. The precise details of this correspondence are determined by the particular jet algorithm being used.

Within the effective field theory there are natural degrees of freedom associated with each region of the two-jet phase space, as indicated in Fig. 1. The complete dijet rate, however, requires integrating over all these regions, and since SCET has no hard cutoff separating soft and collinear degrees of freedom, it would seem that each mode should be integrated over the full QCD phase space (this is the approach followed in [18]). However, this is inconsistent with the effective theory, since, for example, integrating a soft gluon in the collinear region would require it to have momentum well above the cutoff for soft modes in SCET.

Instead, a phase space integral which extends above the cutoff for the relevant mode should be replaced by an ultraviolet divergence, which would then be regulated and renormalized in the usual way. This occurs naturally in SCET because of the multipole expansion for momenta at the vertices. The kinematics for soft and collinear gluon emission is shown in Fig. 2, where $p^\pm$ scale as Q, $p^\perp$ scale as λQ, and the k's scale as $\lambda^2 Q$. Because of the multipole expansion, a given component of momentum is not conserved at vertices involving particles whose typical momenta scale differently with λ. As a consequence, the phase space for each mode in SCET differs from that in full QCD, and it is misleading to use the kinematics in Fig. 1 in the effective theory. For example, in the soft emission graph in Fig. 2, conservation of momentum requires $p_1^- = Q$, $p_2^+ = Q$, while the k's are unconstrained. It is integrals over these unconstrained momenta which will give rise to ultraviolet divergent phase space integrals in the EFT. This is the approach followed in [11], where ultraviolet divergent phase space integrals are obtained for the soft and jet functions at NLO for angularity distributions in SCET. This is also what happens in SCET in loop

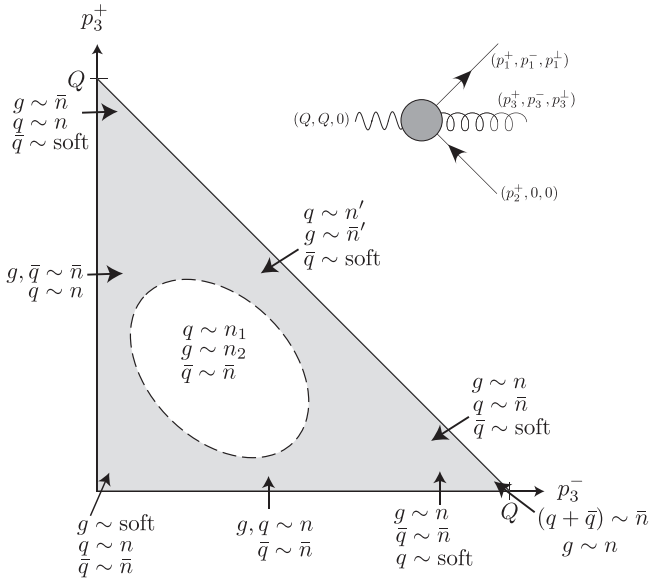

FIG. 1. Three-body phase space in p_3^+, p_3^- variables. The shaded area indicates regions which may be described with two collinear directions in SCET; the white region in the center requires three directions.

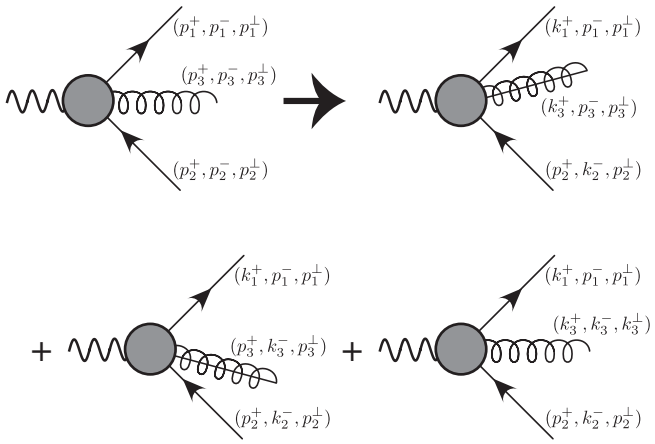

FIG. 2. Kinematics in SCET. In the top right SCET diagram the gluon is n-collinear, in the bottom left it is $\bar{n}$-collinear, and in the bottom right it is soft. Additional diagrams with soft quarks arise at higher order in λ.

graphs, where both soft and collinear degrees of freedom propagate, integrated over the appropriate kinematic variables. Since phase space integrals are just loop graphs with internal propagators placed on shell, the same rules apply.

It is straightforward to illustrate this for various jet definitions. In the SW definition, a two-jet event is defined as one in which all but a fraction β of the total energy of the event is deposited in two back-to-back cones with half angle δ [14]. The JADE algorithm requires that the invariant mass M_{ik}^2 of every pair of final-state partons i and k be calculated. If any are less than a fraction, j, of the total center of mass energy squared, Q^2, then the momenta of the pair with the smallest invariant mass are combined into a single jet according to a recombination scheme which is part of the jet definition, the details of which are not relevant at $O(\alpha_s)$. This process is repeated until no pair has an invariant mass less than jQ^2. The $k_\perp$ algorithm is a modified version of the JADE algorithm which clusters partons based on their relative transverse momentum rather than their invariant mass. The corresponding kinematic variable is

$$y_{ij} = \frac{2}{Q^2}(1 - \cos\theta_{ij}) \min(E_i^2, E_j^2). \tag{2}$$

For massless particles this is equal to

$$y_{ij} = \frac{M_{ij}^2}{Q^2} \min\left(\frac{E_i}{E_j}, \frac{E_j}{E_i}\right). \tag{3}$$

The final states with the smallest y_{ij}, given that it is less than a resolution parameter y_c, are combined according to a combination prescription. This process is repeated until all pairs have $y_{ij} > y_c$. In Fig. 3 we illustrate the two-jet regions in QCD as defined by the JADE, SW, and $k_\perp$ algorithms. The SCET regime for the two-jet cross section corresponds to choosing the parameters δ, β, j, or y_c to be much less than one in the respective jet definition.

For the two-jet JADE cross section, for example, integrating k_3^+ in the soft sector all the way up to Q, as in Fig. 3(a), corresponds to integrating the gluon momentum far above the cutoff. In the EFT, the upper limit of integration should therefore be replaced by an ultraviolet cutoff. Indeed, while the regions of integration for the various jet definitions are quite complicated, as far as the soft gluon is concerned they should have no structure above the soft scale. A similar situation holds for collinear gluons, where the effective cutoffs in the perpendicular and anticollinear directions are parametrically smaller than Q.

At $O(\alpha_s)$, the JADE algorithm corresponds to a cut on the invariant masses M_{ij} of each pair of partons: if $M_{ij}^2 < jQ^2$, the partons are considered to lie in the same jet, and the event is a two-jet event. The constraints in full QCD shown in Fig. 3(a) are

$$\begin{aligned} \frac{M_{qg}^2}{Q^2} &= \frac{p_3^+}{Q - p_3^-} < j, \\ \frac{M_{\bar{q}g}^2}{Q^2} &= \frac{p_3^-}{Q} - \frac{p_3^+ p_3^-}{Q(Q - p_3^-)} < j, \\ \frac{M_{q\bar{q}}^2}{Q^2} &= \frac{Q - p_3^- - p_3^+}{Q} < j. \end{aligned} \tag{4}$$

Expanding these constraints in the n-collinear sector, we find

$$\begin{aligned} \frac{M_{qg}^2}{Q^2} &= \frac{k_3^+}{Q - p_3^-} < j, \\ \frac{M_{\bar{q}g}^2}{Q^2} &= \frac{p_3^-}{Q} < j, \\ \frac{M_{q\bar{q}}^2}{Q^2} &= \frac{Q - p_3^-}{Q} < j \end{aligned} \tag{5}$$

while in the soft sector we obtain

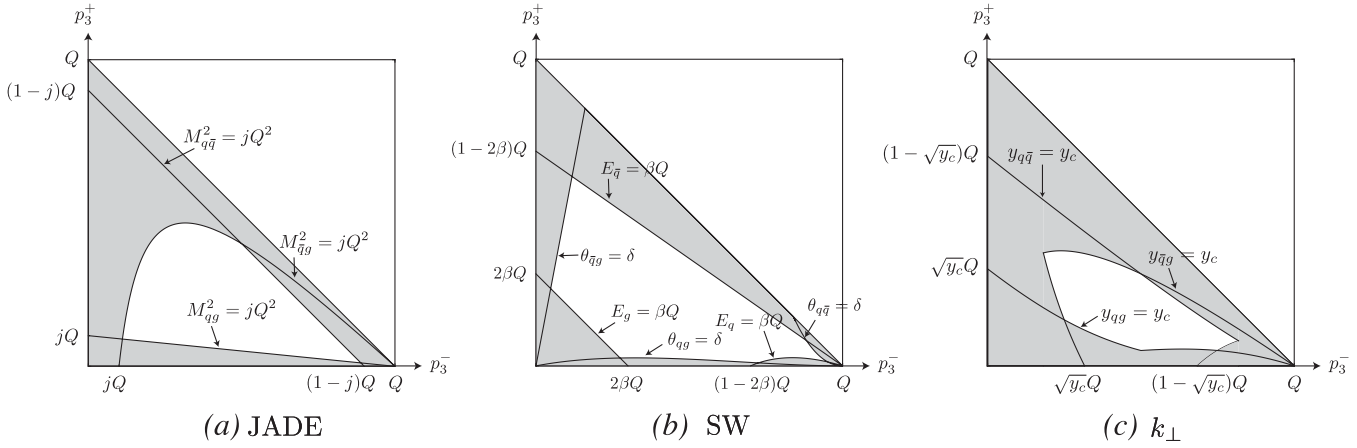

(a) JADE (b) SW (c) $k_\perp$

FIG. 3. Three-body phase space for different jet definitions in QCD. The shaded region corresponds to the two-jet region; the unshaded region in the center is the three-jet region.

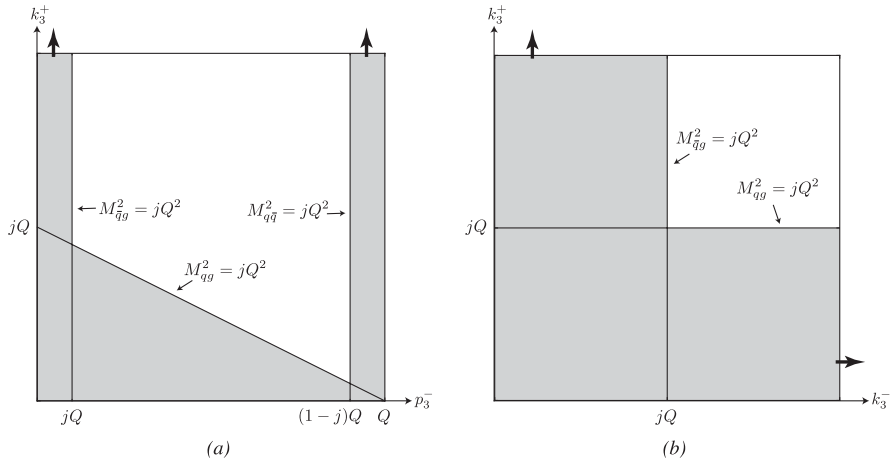

FIG. 4. Phase space corresponding to two-jet events using the JADE algorithm in (a) the n-collinear gluon sector, and (b) the soft gluon and zero-bin sectors. The thick arrows indicate integrations to infinity.

$$\frac{M_{qg}^2}{Q^2} = \frac{k_3^+}{Q} < j, \qquad \frac{M_{\bar{q}g}^2}{Q^2} = \frac{k_3^-}{Q} < j \tag{6}$$

(while the constraint $M_{q\bar{q}}^2 < jQ^2$ is never satisfied). Finally, in order to avoid double-counting of the soft sector, the zero-bin of the collinear region must be subtracted [18]. Taking the soft limit of the n-collinear region in Eq. (5) gives the same region as the soft sector, Eq. (6). The corresponding regions of phase space are shown in Fig. 4(a) and 4(b).

We note that, as required, the phase space contains no explicit reference to any scales above the cutoff of the theory and has no structure above this scale.

Similar constraints in the soft, collinear, and zero-bin sectors are easily obtained for the SW and $k_\perp$ definitions, and are summarized in Table I. Note that in both SW and $k_\perp$, the zero-bin region is not the same as the soft region, since taking the soft limit of the n-collinear phase space is not the same as taking the soft limit of the full QCD phase space. The corresponding regions are illustrated in Figs. 5 and 6.

Note that we have not had to specify the SCET expansion parameter λ in order to expand the phase space in the soft and collinear sectors; we have only assumed that $\lambda \ll 1$ so that the multipole expansion is valid. Similarly, we have not assumed any relative scaling between β and δ in the SW jet definition.

III. DIJET RATES TO $O(\alpha_s)$

In this section we calculate the NLO dijet rate (denoted f_2) in the JADE, SW, and $k_\perp$ schemes in SCET, which is straightforward to do given the phase space regions of the previous section. We show that in each case SCET reproduces full QCD, as it must. We examine the scales that appear in the soft and collinear cross sections, where the power-counting parameter λ is determined by the dynamics in each algorithm. It is instructive to note the cancellation of ultraviolet divergences between the soft and

TABLE I. Two-jet regions of three-body phase space for JADE, Sterman-Weinberg , and $k_\perp$ jet algorithms.

Jet Definition	n-collinear Regions	Soft Regions	Zero-bin Regions
JADE	$k_3^+ < j(Q - p_3^-)$ $p_3^- < jQ$ $p_3^- > Q(1-j)$	$k_3^+ < jQ$ $k_3^- < jQ$	$k_3^+ < jQ$ $k_3^- < jQ$
SW	$k_3^+ < p_3^- \frac{(Q-p_3^-)^2}{Q^2}\delta^2$ $p_3^- < 2\beta Q$ $p_3^- > (1-2\beta)Q$	$\frac{k_3^+}{k_3^+ + k_3^-} < \delta^2$ $\frac{k_3^-}{k_3^+ + k_3^-} < \delta^2$ $k_3^+ + k_3^- < 2\beta Q$	$k_3^+ < \delta^2 p_3^-$ $p_3^- < 2\beta Q$
$k_\perp$	$\min(\frac{k_3^+}{p_3^-}, \frac{k_3^+ p_3^-}{(Q-p_3^-)^2}) < y_c$ $(p_3^-)^2 < y_c Q^2$ $(Q - p_3^-)^2 < y_c Q^2$	$(k_3^+ + k_3^-)k_3^+ < y_c Q^2$ $(k_3^+ + k_3^-)k_3^- < y_c Q^2$	$k_3^+ p_3^- < y_c Q^2$ $(p_3^-)^2 < y_c Q^2$

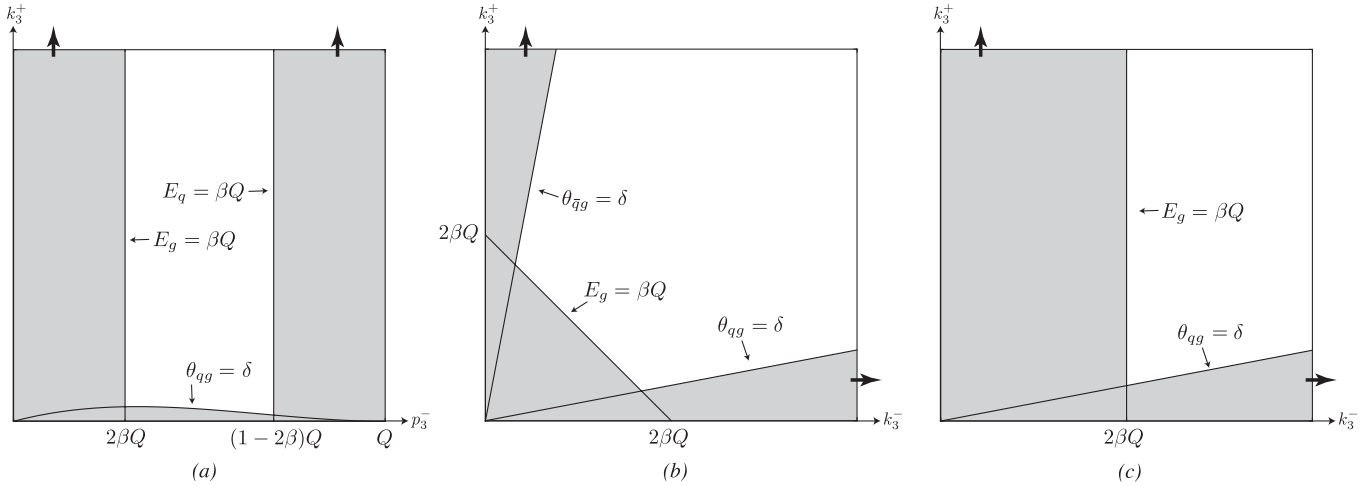

FIG. 5. Phase space corresponding to two-jet events using the SW algorithm in (a) the n-collinear gluon sector, (b) the soft gluon sector, and (c) the zero-bin sector. As before, the thick arrows indicate integrations to infinity.

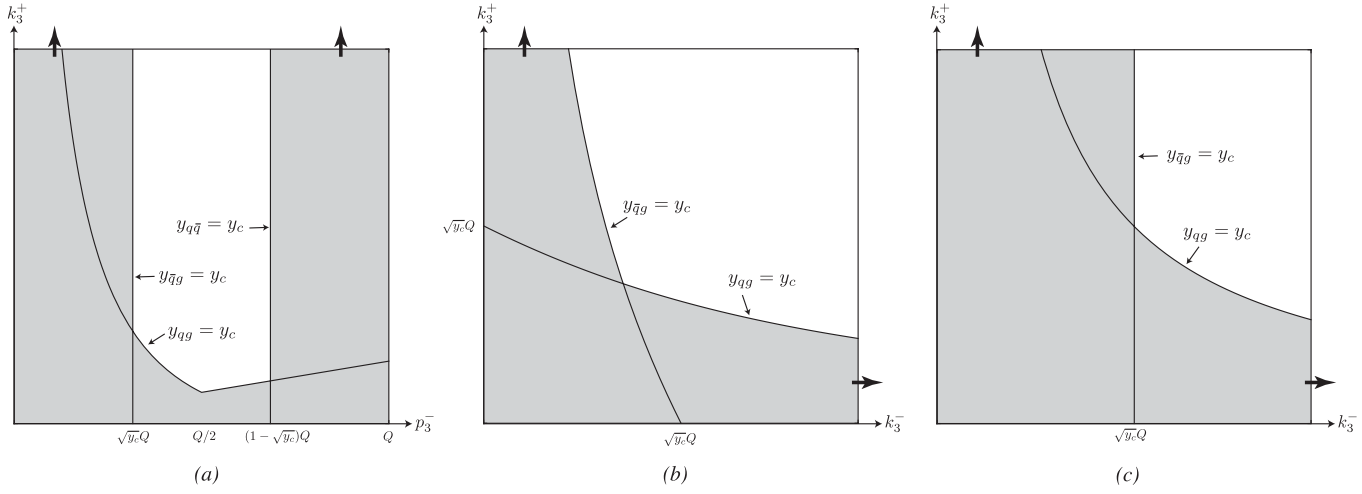

FIG. 6. As in Fig. 5, but using the $k_\perp$ algorithm.

collinear real emission contributions. We also consider the infrared safety of the soft and collinear rates separately.

At $O(\alpha_s)$ the only contribution to the dijet rate comes from the two-jet SCET operator $O_2 = \bar{\xi}_n W_n \gamma^\mu W_{\bar{n}}^\dagger \xi_{\bar{n}}$. The matching calculation from the full QCD current $\bar{\psi}\gamma^\mu\psi$ onto O_2 has been performed many times in the literature [15,19,20], with the Wilson coefficient

$$C_2 = 1 + \frac{\alpha_s C_F}{2\pi}\left(-\frac{1}{2}\ln^2\frac{\mu^2}{-Q^2} - \frac{3}{2}\ln\frac{\mu^2}{-Q^2} - 4 + \frac{\pi^2}{12}\right) \tag{7}$$

and the $\overline{\text{MS}}$ counterterm

$$Z_2 = 1 + \frac{\alpha_s C_F}{2\pi}\left(\frac{1}{\epsilon^2} + \frac{3}{2\epsilon} + \frac{1}{\epsilon}\ln\frac{\mu^2}{-Q^2}\right) \tag{8}$$

where we are working in $d = 4 - 2\epsilon$ dimensions. The SCET differential cross section for soft gluon emission is given by

$$\frac{1}{\sigma_0}d\sigma^s = \frac{\alpha_s C_F}{2\pi}\frac{\mu^{2\epsilon}e^{\epsilon\gamma_E}}{\Gamma(1-\epsilon)}dk_3^+ dk_3^- \frac{2\theta(k_3^+ k_3^-)}{(k_3^+)^{1+\epsilon}(k_3^-)^{1+\epsilon}} \tag{9}$$

while for n-collinear gluon emission it is

$$\frac{1}{\sigma_0}d\sigma^n = \frac{\alpha_s C_F}{2\pi}\frac{\mu^{2\epsilon}e^{\epsilon\gamma_E}}{\Gamma(1-\epsilon)}dk_3^+ dp_3^- \frac{(p_3^- k_3^+)^{-\epsilon}}{Qk_3^+} \times\left(\frac{p_3^-}{Q}(1-\epsilon) + 2\frac{Q-p_3^-}{p_3^-}\right) \tag{10}$$

where $\sigma_0 = (4\pi\alpha^2/Q^2)\sum_f e_f^2$ is the leading order Born cross section with a sum over the (anti-)quark charges e_f. The dependence on $\vec{k}_3^\perp$ and $\vec{p}_3^\perp$ has been eliminated via the gluon on-shell condition, and the integral over the $2-2\epsilon$

perpendicular components of the gluon momentum has been performed in each case.

Finally, the differential rate in the gluon zero-bin region, $d\sigma^{n0}$, is obtained by taking the soft limit of Eq. (10), which is the same as the soft rate,

$$d\sigma^{n0} = d\sigma^{s}. \tag{11}$$

(There are also zero-bin regions corresponding to the quark and antiquarks becoming soft, but they are higher order in λ and we will not consider them here.) For the n-collinear region there are two zero-bins: $p_3^- \to 0$ and $p_1^- \to 0$, but the contribution to the cross section from the latter is of higher order in λ and so we will not consider them here.

A. JADE

Integrating the soft rate over the soft dijet region (6) in the JADE definition gives

$$\frac{1}{\sigma_0}\sigma^{s}_{\rm JADE} = \frac{\alpha_s C_F}{2\pi}\left(-\frac{2}{\epsilon^2} - \frac{2}{\epsilon}\ln\frac{\mu^2}{j^2Q^2} - \ln^2\frac{\mu^2}{j^2Q^2} + \frac{\pi^2}{6}\right) \tag{12}$$

where we have taken $j \ll 1$ and kept only the leading terms in j. Integrating the n-collinear rate over the region (5), we find

$$\frac{1}{\sigma_0}\tilde{\sigma}^{n}_{\rm JADE} = \frac{\alpha_s C_F}{2\pi}\left(\frac{3}{2\epsilon} + \frac{2}{\epsilon}\ln j + \frac{3}{2}\ln\frac{\mu^2}{jQ^2} + 2\ln\frac{\mu^2}{Q^2}\ln j - 3\ln^2 j - \frac{\pi^2}{3} + \frac{7}{2}\right) \tag{13}$$

where the tilde denotes that the zero-bin has not been subtracted. The rate in the zero-bin region is identical to that in the soft region, and so the zero-bin subtracted result for the emission of an n-collinear gluon is

$$\begin{aligned}\frac{1}{\sigma_0}\sigma^{n}_{\rm JADE} &= \frac{1}{\sigma_0}(\tilde{\sigma}^{n}_{\rm JADE} - \sigma^{n0}_{\rm JADE}) = \frac{1}{\sigma_0}(\tilde{\sigma}^{n}_{\rm JADE} - \sigma^{s}_{\rm JADE}) \\ &= \frac{\alpha_s C_F}{2\pi}\left(\frac{2}{\epsilon^2} + \frac{3}{2\epsilon} + \frac{2}{\epsilon}\ln\frac{\mu^2}{jQ^2} + \frac{3}{2}\ln\frac{\mu^2}{jQ^2} + \ln^2\frac{\mu^2}{jQ^2} - \frac{\pi^2}{2} + \frac{7}{2}\right).\end{aligned} \tag{14}$$

The emission of a collinear gluon in the $\bar{n}$ direction, i.e. from the antiquark, can be calculated in a similar way, and it gives the same contribution.

In pure dimensional regularization, all the virtual vertex corrections and the wave function renormalizations involve scaleless integrals and thus vanish. Hence we only need to add up the real emission contributions:

$$\begin{aligned}\frac{1}{\sigma_0}\sigma^{R}_{\rm JADE} &= \frac{1}{\sigma_0}((\tilde{\sigma}^{n}_{\rm JADE} - \sigma^{n0}_{\rm JADE}) + (\tilde{\sigma}^{\bar{n}}_{\rm JADE} - \sigma^{\bar{n}0}_{\rm JADE}) + \sigma^{s}_{\rm JADE}) \\ &= \frac{1}{\sigma_0}(\tilde{\sigma}^{n}_{\rm JADE} + \tilde{\sigma}^{\bar{n}}_{\rm JADE} - \sigma^{s}_{\rm JADE}) \\ &= \frac{\alpha_s C_F}{2\pi}\left(\frac{2}{\epsilon^2} + \frac{3}{\epsilon} + \frac{2}{\epsilon}\ln\frac{\mu^2}{Q^2} - 2\ln^2 j + \ln^2\frac{\mu^2}{Q^2} + 3\ln\frac{\mu^2}{jQ^2} - \frac{5\pi^2}{6} + 7\right).\end{aligned} \tag{15}$$

Note that the soft contribution enters into the final expression with a minus sign. This is a consequence of zero-bin subtraction and the fact that zero-bins are identical to the soft contribution. Similar observations have been pointed out in [21–23]. The divergent terms in Eq. (15) are cancelled by the counterterm $|Z_2|^2$, and including the Wilson coefficient, $|C_2|^2$, gives the two-jet fraction

$$\begin{aligned}f_2^{\rm JADE} &= \frac{|C_2|^2}{|Z_2|^2}\left(1 + \frac{1}{\sigma_0}(\sigma^{n}_{\rm JADE} + \sigma^{\bar{n}}_{\rm JADE} + \sigma^{s}_{\rm JADE})\right) \\ &= 1 + \frac{\alpha_s C_F}{2\pi}\left(-2\ln^2 j - 3\ln j + \frac{\pi^2}{3} - 1\right).\end{aligned} \tag{16}$$

This result agrees with the full QCD calculation given in [24,25].

It is instructive to comment on a few details of the SCET result. First of all, since dimensional regularization regulates both the infrared and ultraviolet divergences, the cancellation of ultraviolet divergences between the soft and collinear emissions is not explicit. To show how this works, we can repeat the calculation with the quark and antiquark offshell, p_1^2, $p_2^2 \sim \lambda^2 \neq 0$, so that all $1/\epsilon$ divergences in the calculation are ultraviolet. The calculation is given in the Appendix. The resulting rate for soft gluon emission over the JADE phase space is

$$\begin{aligned}\frac{1}{\sigma_0}\sigma^{s}_{\rm JADE} = \frac{\alpha_s C_F}{2\pi}\Bigg(&-\frac{2}{\epsilon}\left(\ln\frac{p_1^2}{jQ^2} + \ln\frac{p_2^2}{jQ^2}\right) + \left(\ln\frac{p_1^2}{Q^2} + \ln\frac{p_2^2}{Q^2}\right)^2 - 2\left(\ln\frac{p_1^2}{Q^2} + \ln\frac{p_2^2}{Q^2}\right)\ln\frac{\mu^2}{Q^2} \\ &+ \cdots\Bigg)\end{aligned} \tag{17}$$

where the ellipses denote finite constant terms which are not relevant for the discussion. The unsubtracted n-collinear cross section is

$$\frac{1}{\sigma_0}\tilde{\sigma}^{n}_{\rm JADE} = \frac{\alpha_s C_F}{2\pi}\left(-\frac{2}{\epsilon^2} + \frac{2}{\epsilon}\left(\ln\frac{p_1^2}{jQ^2} - \ln\frac{\mu^2}{j^2Q^2}\right) - \ln^2\frac{p_1^2}{Q^2} + 2\ln\frac{\mu^2}{Q^2}\ln\frac{p_1^2}{Q^2} + \frac{3}{2}\ln\frac{p_1^2}{Q^2}\right) + \ldots \tag{18}$$

while the zero-bin region gives

$$\frac{1}{\sigma_0}\sigma^{n0}_{\rm JADE} = \frac{\alpha_s C_F}{2\pi}\left(-\frac{2}{\epsilon^2} - \frac{2}{\epsilon}\ln\frac{\mu^2}{j^2Q^2}\right) + \ldots. \quad (19)$$

Thus, the zero-bin subtracted n-collinear cross section is

$$\frac{1}{\sigma_0}\sigma^{n}_{\rm JADE} = \frac{\alpha_s C_F}{2\pi}\left(\frac{2}{\epsilon}\ln\frac{p_1^2}{jQ^2} - \ln^2\frac{p_1^2}{Q^2} + 2\ln\frac{\mu^2}{Q^2}\ln\frac{p_1^2}{Q^2} + \frac{3}{2}\ln\frac{p_1^2}{Q^2}\right) + \ldots. \quad (20)$$

The result for $\bar{n}$-collinear gluon emission will be the same as that for n-collinear gluon emission with the replacement $p_1^2 \to p_2^2$. Note that the $1/\epsilon^2$ divergence from collinear emission is removed by the zero-bin. Combining the real emission contributions to the JADE cross section, Eq. (21), we see that while the phase space integrals for soft and collinear gluon emission are individually ultraviolet divergent, with mixed ultraviolet infrared divergent terms, the ultraviolet divergences cancel in the sum:

$$\frac{1}{\sigma_0}\sigma^{R}_{\rm JADE} = \frac{\alpha_s C_F}{2\pi}\left(2\ln\frac{p_1^2}{Q^2}\ln\frac{p_2^2}{Q^2} + \frac{3}{2}\ln\frac{p_1^2}{Q^2} + \frac{3}{2}\ln\frac{p_2^2}{Q^2}\right) + \ldots. \quad (21)$$

This is the same cancellation which occurs at the one-loop level in SCET [1], in which separately ultraviolet and infrared divergent terms cancel in the sum of the soft and collinear graphs.

The soft and collinear sectors are also individually infrared finite for the JADE algorithm. The soft virtual vertex correction is given by [20], and contributes equally to the two-jet rate in all definitions

$$\frac{1}{\sigma_0}\sigma^{s}_{V} = \frac{\alpha_s C_F}{2\pi}\left(-\frac{2}{\epsilon^2} - \frac{2}{\epsilon}\ln\left(-\frac{\mu^2Q^2}{p_1^2p_2^2}\right) - \ln^2\left(-\frac{\mu^2Q^2}{p_1^2p_2^2}\right)\right) + \ldots. \quad (22)$$

The soft wave function renormalization graphs are zero and so the cross section in the soft sector is given by

$$\frac{1}{\sigma_0}(\sigma^{s}_{\rm JADE} + \sigma^{s}_{V}) = \frac{\alpha_s C_F}{2\pi}\left(-\frac{2}{\epsilon^2} - \frac{4}{\epsilon}\ln\frac{\mu}{jQ}\right) + \ldots. \quad (23)$$

The result is purely ultraviolet divergent and agrees with the pure dimensional regularization calculation in Eq. (12). The collinear contribution is similarly free of infrared divergences.

Second, we note that the scale at which the logarithms in the NLO n-collinear rate are minimized, $\mu = \sqrt{j}Q$, determines the collinear or jet scale in SCET, λQ, and that without the zero-bin subtraction there is no value of μ at which the logarithms in Eq. (13) are minimized. The logarithms in the soft rate (12) are minimized at $\mu = jQ$, the expected soft scale in SCET, $\lambda^2 Q$. From Fig. 4 we see that jQ is the relevant soft scale that emerges from the multipole expansion of the JADE phase space constraints. However, as we shall see from the SW two-jet soft rate, this is not universally the case. The true soft scale depends on the details of the soft theory, which is not addressed here. Furthermore the calculation of the leading logarithmic contribution in full QCD [25,26] shows that the resummed result is not simply given by the exponentiation of the NLO term. It has been demonstrated that the emission of two soft gluons with large angular separation can be combined to constitute a third jet in the JADE clustering algorithm. These types of configurations change the leading-logarithmic two-jet fraction and spoil naïve exponentiation, as the emission of subsequent soft gluons qualitatively changes the phase space constraints. These configurations also involve the parametrically lower scale j^2Q [26], which complicates the summing of logarithms of j. However, this effect does not arise until $O(\alpha_s^2)$, which is beyond the order to which we are working.

Finally, it is instructive to look more closely at the zero-bin subtractions in different regions of phase space. In particular, while the n-collinear region of integration naturally describes the region where the n-collinear quark and gluon form a jet (see Fig. 4(a)), it also includes regions where the antiquark and the gluon, as well as the quark and the antiquark, form jets. In order for an n-collinear gluon to form a jet with an $\bar{n}$-collinear antiquark, the gluon must be soft, and as a result one would expect the entire contribution from this region of phase space to be cancelled by the zero-bin subtraction. Similarly, the region where the n-collinear quark and $\bar{n}$-collinear antiquark form a jet should be cancelled by the corresponding quark and antiquark zero-bins; however, these are subleading in j. We show below that this is indeed the case at $O(\alpha_s)$.[2]

The region where the n-collinear gluon and $\bar{n}$-collinear quark form a jet in the JADE algorithm is defined by the region

$$k_3^+ > p_3^- \frac{(Q - p_3^-)}{Q}, \qquad 0 < p_3^- < jQ \quad (24)$$

and integrating the differential rate (10) over this region gives

$$\frac{\alpha_s C_F}{2\pi}\left(-\frac{1}{\epsilon^2} - \frac{2}{\epsilon}\ln\frac{\mu}{jQ} + \frac{\pi^2}{12} - 2\ln^2\frac{\mu}{jQ}\right) \quad (25)$$

where, as usual, we have dropped terms subleading in j. The zero-bin constraints for the same jet are

$$k_3^+ > k_3^-, \qquad 0 < k_3^- < jQ \quad (26)$$

and integrating the differential rate (11) over this region and expanding in j gives the same result as (25). Hence this region is entirely zero-bin and is absent from the n-collinear rate, thereby reducing the combinations of partons that need to be considered. Similarly, the region where the quark and antiquark form a jet is

[2]We thank S. Freedman for this observation.

$$k_3^+ > \frac{(Q-p_3^-)^2}{Q}, \qquad Q(1-j) < p_3^- < Q \tag{27}$$

and integrating Eq. (11) over this region gives a result of order j, and so the rate vanishes to the order we are working. We expect that such cancellations will continue beyond leading order, simplifying the combinatorics of clustering multigluon states.

B. Sterman-Weinberg and $k_\perp$ jet definitions

It is straightforward to repeat the calculations of the previous section for the SW and $k_\perp$ jet definitions. However, each of these algorithms introduces additional features not present in the JADE calculation: the relevant scales are different and in both cases the zero-bin contribution is distinct from the soft contribution. Furthermore, in the $k_\perp$ definition the soft and collinear rates are not individually infrared safe using dimensional regularization to regulate the ultraviolet, indicating that the rate does not factorize into well-defined soft and collinear contributions in this scheme in SCET.

1. SW

Jets in the SW definition were studied in SCET in [8,9,15]. In these papers it was argued that because the kinematic cuts on the soft phase space were much larger than the typical soft scale, the soft phase space integral should be unrestricted. In [8,9] this is because the scaling $\beta \sim \delta$ is chosen, while in [15] β is taken to be of order δ^2, but the soft scale is taken to be $\Lambda_{\rm QCD}$. Our results differ, as we have not assumed any relative scaling between βQ, δQ, and $\Lambda_{\rm QCD}$, and we argue that SCET power counting uniquely requires the restricted soft phase space in Fig. 5(b). (We expect, however, that if $\beta \sim \delta$, SCET should be matched at a lower scale onto a new effective theory with unrestricted soft phase space.)

Integrating the differential cross section in Eq. (9) over the phase-space generated by the corresponding constraints, we find

$$\frac{1}{\sigma_0}\sigma^s_{\rm SW} = \frac{\alpha_s C_F}{2\pi}\left(\frac{4}{\epsilon}\ln\delta - 4\ln^2\delta + 8\ln\delta\ln\frac{\mu}{2\beta Q} - \frac{\pi^2}{3}\right). \tag{28}$$

By introducing quark and antiquark off shellnesses as we did for the JADE algorithm, it can be shown that the total soft contribution, $(\sigma^s_{\rm SW}+\sigma^s_V)/\sigma_0$, is infrared finite, and the $1/\epsilon$ terms are ultraviolet divergences. The logarithms in Eq. (28) cannot be minimized for any choice of μ since there is a large $\ln\delta$ in the $1/\epsilon$ term. (See, however, [27] in which factorization and resummation in the SW two-jet rate were studied in perturbative QCD.)

Integrating Eq. (10) over the phase space given by the collinear SW constraints, we find the naïve n-collinear contribution to be

$$\frac{1}{\sigma_0}\tilde\sigma^n_{\rm SW} = \frac{\alpha_s C_F}{2\pi}\left(\frac{1}{\epsilon}\left(\frac{3}{2}+2\ln 2\beta\right)+3\ln\frac{\mu}{\delta Q} + 2\ln 2\beta\ln\frac{\mu^2}{2\beta\delta^2Q^2}+\frac{13}{2}-\frac{2\pi^2}{3}\right). \tag{29}$$

Note that there is no reasonable scale μ at which all the logarithms are minimized. We now need to subtract the $p_3^- \to 0$ zero-bin of the SW n-collinear contribution. Integrating over the relevant phase space gives us

$$\frac{1}{\sigma_0}\sigma^{n0}_{\rm SW} = \frac{\alpha_s C_F}{2\pi}\left(-\frac{1}{\epsilon^2}-\frac{2}{\epsilon}\ln\frac{\mu}{2\beta\delta Q}-2\ln^2\frac{\mu}{2\beta\delta Q}+\frac{\pi^2}{12}\right). \tag{30}$$

The zero-bin gives a nontrivial contribution that is not equal to the soft contribution, because the region of integration generated by taking the collinear and then soft limit is not the same as taking the soft limit of the QCD SW phase space. It is interesting to note that the scale in the n-collinear zero-bin, $\beta\delta Q$, corresponds to the $p_\perp$ of a parton at the edge of the cone with the maximum energy allowed outside the cone, βQ. This corresponds to the intersection point of Fig. 5(c), generated by a consistent expansion of phase space constraints in the effective theory.

The zero-bin subtracted result for the n-collinear sector is

$$\frac{1}{\sigma_0}(\tilde\sigma^n_{\rm SW}-\sigma^{n0}_{\rm SW}) = \frac{\alpha_s C_F}{2\pi}\left(\frac{1}{\epsilon^2}+\frac{3}{2\epsilon}+\frac{2}{\epsilon}\ln\frac{\mu}{\delta Q}+3\ln\frac{\mu}{\delta Q} + 2\ln^2\frac{\mu}{\delta Q}-\frac{3\pi^2}{4}+\frac{13}{2}\right) \tag{31}$$

where the logarithms are now minimized at $\mu=\delta Q$, unlike in Eq. (29). The collinear scale, δQ, corresponds to the $p_\perp$ of a parton at the edge of the cone with typical collinear energy $O(Q)$. The emission of a collinear gluon in the $\bar n$ direction, i.e. from the antiquark, gives the same result.

The n-collinear rate is independent of the jet parameter β, because the phase space region in Fig. 5(b) with a collinear gluon outside the cone with energy less than βQ, where $\beta \ll 1$, corresponds to the zero-bin. This contribution is entirely removed by the zero-bin subtraction and Eq. (31) is given only by the region where the n-collinear quark and gluon lie in the cone. This underscores the consistency of the phase space expansion in Sec. II and the zero-bin prescription. The soft sector resolves the cone in addition to the scale βQ and gives rise to the double logarithm cross term in the SW result below.

Combining these results gives

$$f_2^{\mathrm{SW}} = \frac{|C_2|^2}{|Z_2|^2}\left(1 + \frac{2}{\sigma_0}(\tilde{\sigma}^n_{\mathrm{SW}} - \sigma^{n0}_{\mathrm{SW}}) + \frac{1}{\sigma_0}\sigma^s_{\mathrm{SW}}\right) = 1 + \frac{\alpha_s C_F}{\pi}\left(-4\ln 2\beta \ln\delta - 3\ln\delta - \frac{\pi^2}{3} + \frac{5}{2}\right) \tag{32}$$

in agreement with the full QCD calculation [14].

2. $k_\perp$

The $k_\perp$ two-jet rate in SCET reveals a more subtle cancellation of divergences than the previous two algorithms and highlights again the importance of zero-bin subtractions. Integrating the differential cross section for the emission of a soft gluon over the soft phase space in Fig. 6(b), we find that $\sigma^s_{k_\perp}$ is not regulated in dimensional regularization. Performing the k_3^+ integral first over the $\bar{q}g$ jet region of phase space, we obtain a term proportional to

$$\frac{d\sigma^s_{k_\perp}}{dk_3^-} \propto \frac{(Q^2 y_c - (k_3^-)^2)^{-\epsilon}}{\epsilon k_3^-} + \cdots, \tag{33}$$

where the ellipses denote terms which are finite in $d = 4 - 2\epsilon$ dimensions. This term causes the k_3^- integration to diverge at zero. A similar problem arises when integrating over the soft region generated by the qg jet constraint. Despite this divergence, the total two-jet cross section is finite in QCD and so must be finite in SCET. The region that gives rise to this divergence is also integrated over in the zero-bin calculations and since the soft and zero-bin integrands are the same the divergence cancels in the difference. Integrating the soft differential rate over the combined soft and zero-bin regions gives a finite result in d dimensions:

$$\frac{1}{\sigma_0}(\sigma^s_{k_\perp} - \sigma^{n0}_{k_\perp} - \sigma^{\bar{n}0}_{k_\perp}) = \frac{\alpha_s C_F}{2\pi}\left(\frac{2}{\epsilon^2} + \frac{2}{\epsilon}\ln\frac{\mu^2}{y_c Q^2} + \ln^2\frac{\mu^2}{y_c Q^2} - \frac{\pi^2}{3}\right) \tag{34}$$

where we see the soft scale $\sqrt{y_c}Q$ appear as in Fig. 6. We combine this with the rate to produce an n-collinear gluon,

$$\frac{1}{\sigma_0}\tilde{\sigma}^n_{k_\perp} = \frac{\alpha_s C_F}{2\pi}\left(\frac{1}{\epsilon}\left(\frac{3}{2} + \ln y_c\right) + \ln\frac{\mu^2}{y_c Q^2}\left(\frac{3}{2} + \ln y_c\right) - 3\ln 2 - \frac{\pi^2}{3} + \frac{7}{2}\right) \tag{35}$$

to obtain the total two-jet rate for emission of a real gluon

$$\frac{1}{\sigma_0}(\tilde{\sigma}^n_{k_\perp} + \tilde{\sigma}^{\bar{n}}_{k_\perp} + \sigma^s_{k_\perp} - \sigma^{n0}_{k_\perp} - \sigma^{\bar{n}0}_{k_\perp}) = \frac{\alpha_s C_F}{2\pi}\left(\frac{2}{\epsilon^2} + \frac{1}{\epsilon}\left(2\ln\frac{\mu^2}{Q^2} + 3\right) + \ln^2\frac{\mu^2}{Q^2} + 3\ln\frac{\mu^2}{Q^2} - \ln^2 y_c - 3\ln y_c - 6\ln 2 - \pi^2 + 7\right) \tag{36}$$

where again n and $\bar{n}$ collinear gluon emission give the same contribution and the virtual piece vanishes. Including the counterterm Z_2 and the Wilson coefficient C_2, we reproduce the known NLO $k_\perp$ result [25]

$$f_2^{k_\perp} = 1 + \frac{\alpha_s C_F}{2\pi}\left(-\ln^2 y_c - 3\ln y_c - 6\ln 2 + \frac{\pi^2}{6} - 1\right). \tag{37}$$

This calculation reemphasizes the importance of zero-bin subtraction: without it, the evaluation of a finite $f_2^{k_\perp}$ would not be possible. Since the soft and collinear cross sections are not regulated in dimensional regularization, it is useful to regulate the infrared and ultraviolet divergences separately by taking the outgoing quark and antiquark off shell. The resulting rate for soft gluon emission then becomes

$$\frac{1}{\sigma_0}\sigma^s_{k_\perp} = \frac{\alpha_s C_F}{2\pi}\ln^2\frac{p_1^2 p_2^2}{Q^4 y_c} + \ldots. \tag{38}$$

Note that unlike the previous algorithms, the soft real emission result is not ultraviolet divergent. Combining this with the contribution from the soft virtual vertex correction (22) gives

$$\frac{1}{\sigma_0}(\sigma^s_{k_\perp} + \sigma^s_V) = \frac{\alpha_s C_F}{2\pi}\left(-\frac{2}{\epsilon^2} - \frac{2}{\epsilon}\ln\frac{\mu^2 Q^2}{p_1^2 p_2^2} + 2\ln\frac{p_1^2 p_2^2}{Q^4}\ln\frac{\mu^2}{y_c Q^2}\right) + \ldots. \tag{39}$$

This shows explicitly that the rate in the soft sector is not infrared safe.

The rate for n-collinear gluon emission and the zero-bin are, respectively,

$$\frac{1}{\sigma_0}\tilde{\sigma}^n_{k_\perp} = \frac{\alpha_s C_F}{2\pi}\left(-\frac{2}{\epsilon^2} - \frac{2}{\epsilon}\ln\frac{\mu^2}{p_1^2\sqrt{y_c}} - \ln^2\frac{\mu^2}{p_1^2} + \frac{3}{2}\ln\frac{p_1^2}{Q^2 y_c}\right) + \ldots$$

$$\frac{1}{\sigma_0}\sigma^{n0}_{k_\perp} = \frac{\alpha_s C_F}{2\pi}\left(-\frac{2}{\epsilon^2} - \frac{2}{\epsilon}\ln\frac{\mu^2}{p_1^2\sqrt{y_c}} + \ln^2\frac{p_1^2}{y_c Q^2} - \ln^2\frac{\mu^2}{p_1^2}\right) + \ldots. \tag{40}$$

and their difference gives us the zero-bin subtracted result

$$\frac{1}{\sigma_0}\sigma^n_{k_\perp} = \frac{\alpha_s C_F}{2\pi}\left(-\ln^2\frac{p_1^2}{y_c Q^2} + \frac{3}{2}\ln\frac{p_1^2}{y_c Q^2}\right) + \ldots. \tag{41}$$

As with the soft sector, the phase space integration for the n-collinear real emission is ultraviolet finite but infrared

divergent. Combining the real emission contributions to the $k_\perp$ two-jet cross section, we find

$$\frac{1}{\sigma_0}\sigma^R_{k_\perp} = \frac{1}{\sigma_0}(\sigma^n_{k_\perp} + \sigma^{\bar n}_{k_\perp} + \sigma^s_{k_\perp}) = \frac{\alpha_s C_F}{2\pi}\left(\frac{3}{2}\left(\ln\frac{p_1^2}{Q^2} + \ln\frac{p_2^2}{Q^2}\right) + 2\ln\frac{p_1^2}{Q^2}\ln\frac{p_2^2}{Q^2}\right) + \ldots. \tag{42}$$

The infrared divergences in Eq. (42) are completely cancelled by the total virtual contribution σ_V given in Eq. (A10). As expected, the virtual graphs convert the infrared divergences in the real emission diagrams into ultraviolet ones. While SCET reproduces the known NLO $k_\perp$ result, the soft and collinear rates are not independently infrared safe, indicating for the $k_\perp$ phase space the soft and collinear modes do not factorize in SCET using dimensional regularization to regulate the ultraviolet.

IV. FACTORIZATION AND SCHEME DEPENDENCE

It is useful to examine the failure of SCET to factorize the $k_\perp$ rate into separately infrared safe soft and collinear pieces, particularly given the fact that the regions of integration for the soft gluons are quite similar in the infrared between $k_\perp$ and JADE. Instead, the bad behavior in Eq. (33) comes from the region of large k^+ and small k^- and vice-versa—a region which is infrared divergent, but sensitive to the ultraviolet regulator. Since, as we have shown, the ultraviolet divergences in the phase space integrals cancel between the soft and collinear degrees of freedom, this is an unphysical region, and so cancels from the total rate. The same cancellation occurs at the one-loop level, in which terms of order $1/\epsilon_{\rm UV}\ln p_i^2$ cancel between soft and collinear graphs [1]. However, this unphysical region can also be eliminated by defining the soft function with a cutoff Λ_f. In particular, we show in this section that while the $k_\perp$ algorithm in dimensional regularization does not factorize in SCET into separate infrared safe contributions, regulating the ultraviolet with a cutoff on the light-cone components of the gluon momentum,

$$|k^+| < \Lambda_f, \qquad |k^-| < \Lambda_f \tag{43}$$

results in an infrared safe soft function.

Integrating the soft rate over the relevant region for $k_\perp$, including the cutoff (43), and continuing to work in d dimensions to regulate the infrared, we find for real soft gluon emission

$$\frac{1}{\sigma_0}\sigma^s_{k_\perp} = \frac{\alpha_s C_F}{2\pi}\left(\frac{2}{\epsilon^2} + \frac{2}{\epsilon}\ln\frac{\mu^2}{\Lambda_f^2} - \ln^2\frac{y_c Q^2}{\Lambda_f^2} + \ln^2\frac{\mu^2}{\Lambda_f^2} - \frac{\pi^2}{3}\right). \tag{44}$$

Similarly, the same regulator for soft real gluon emission in the JADE algorithm gives

$$\frac{1}{\sigma_0}\sigma^s_{\rm JADE} = \frac{\alpha_s C_F}{2\pi}\left(\frac{2}{\epsilon^2} + \frac{2}{\epsilon}\ln\frac{\mu^2}{\Lambda_f^2} - \frac{1}{2}\ln^2\frac{j^2Q^2}{\Lambda_f^2} + \ln^2\frac{\mu^2}{\Lambda_f^2} - \frac{\pi^2}{6}\right). \tag{45}$$

Note that with a cutoff, the $1/\epsilon^2$ and Sudakov double logs $\ln^2 j$ and $\ln^2 y_c$ are entirely contained within the soft function, as opposed to pure dimensional regularization, in which the collinear graphs also contain double logs. This is in agreement with [25,26], where the Sudakov logs are calculated entirely from the soft graphs.

The soft virtual vertex correction with a cutoff of Λ_f in $|k^+|$ and $|k^-|$ gives a modified vertex correction

$$\sigma^s_V = \frac{\alpha_s C_F}{2\pi}\left(-\frac{2}{\epsilon^2} - \frac{2}{\epsilon}\ln\frac{\mu^2}{\Lambda_f^2} - \ln^2\frac{\mu^2}{\Lambda_f^2} + \frac{\pi^2}{6}\right) \tag{46}$$

giving the finite results

$$\frac{1}{\sigma_0}(\sigma^s_{k_\perp} + \sigma^s_V) = -\frac{\alpha_s C_F}{2\pi}\left(\ln^2\frac{y_c Q^2}{\Lambda_f^2} + \frac{\pi^2}{6}\right).$$
$$\frac{1}{\sigma_0}(\sigma^s_{\rm JADE} + \sigma^s_V) = -\frac{\alpha_s C_F}{4\pi}\ln^2\frac{j^2Q^2}{\Lambda_f^2}. \tag{47}$$

Note that the infrared divergences cancel between the real and virtual graphs, and that there are no large logs in the soft function for Λ_f of order the relevant soft scale, jQ or $\sqrt{y_c}Q$.

These results demonstrate the fact that factorization of rates in SCET into soft and collinear components is scheme-dependent. Such dependence on infrared regulators was also noted in a different context in [11,28]. Using the method introduced in [11] to test infrared safety at one-loop, one would conclude that the soft contribution to the $k_\perp$ rate is infrared divergent. This differs from our results, because, as we have shown, the infrared safety of the soft function is ultraviolet regulator dependent. Introducing a cutoff removes the unphysical region of $k^\pm \to 0$ and $k^\mp \to \infty$ and results in an infrared safe soft contribution to the two-jet $k_\perp$ rate.[3] The bad behavior of $k_\perp$ in dimensional regularization in SCET is therefore a feature of dimensional regularization, not of SCET. The factorization for jet rates depends on the ultraviolet regulator of the theory as well as the infrared.

V. CONCLUSION

We have presented a consistent treatment of phase space integrals over soft and collinear degrees of freedom in SCET, illustrating this with the explicit example of the NLO dijet rate for three different jet algorithms. In this

[3]Similarly, the NLO soft function for angularities, τ_a, for $1 < a < 2$ integrated over τ_a between 0 and 1 can be shown to be infrared finite if defined with an ultraviolet cutoff.

approach the phase space for different modes in the effective theory are insensitive to details above their cutoff, giving real emission contributions with ultraviolet divergences which cancel between the collinear and soft sectors. Although the leading order SCET Lagrangian separates soft and collinear modes and the differential cross section has been shown to factorize, we demonstrated that using dimensional regularization the $k_\perp$ algorithm does not factorize into infrared safe soft and collinear rates. We showed that this is related to a divergence in an unphysical region which cancels between the soft and collinear sectors, and is sensitive to the ultraviolet regulator.

Zero-bin subtraction is necessary to consistently integrate over the phase space configurations that need to be considered in a given jet algorithm. The zero-bin subtraction was shown to entirely remove regions of the naïve collinear rate where n and $\bar{n}$ collinear degrees of freedom form a jet at NLO in the JADE algorithm and for collinear partons outside the cone in SW. The $k_\perp$ and SW dijet rates provide nontrivial examples of zero-bin subtraction, which are different from the soft contribution.

We have not attempted to sum logarithms of the small jet parameters at this stage. While the running of C_2 makes summing some of the logarithms straightforward, the soft physics in these theories is more complicated. For example, the JADE algorithm is known not to exponentiate: there are three-jet configurations which contribute at $O(\alpha_s^2 \ln^4 j)$ in which two gluons, which would naïvely be unresolved from the quarks, are combined to form a third jet [26]. Such configurations have no simple relation to the one-gluon phase space and are not obtained by exponentiating the one-loop result. From an effective field theory viewpoint, these configurations also involve the scale $j^2 Q$, which is parametrically smaller than the soft scale jQ. The soft function for the SW algorithm, in contrast, naïvely has an anomalous dimension of order $\ln\delta$, and so large logarithms of δ cannot be resummed in this formulation of the low-energy theory.

ACKNOWLEDGMENTS

We thank A. Blechman, C. Bauer, S. Freedman, Z. Ligeti, A. Manohar, I. Rothstein, and M. Trott for useful discussions and comments on the manuscript. This work was supported by the Natural Sciences and Engineering Research Council of Canada.

APPENDIX A: OFF SHELL CALCULATIONS

The SCET differential cross section for soft gluon emission and off shell quarks, $p_1^2,\ p_2^2 \neq 0$, is

$$\frac{1}{\sigma_0} d\sigma^s = \frac{\alpha_s C_F}{2\pi} \frac{\mu^{2\epsilon} e^{\epsilon\gamma_E}}{\Gamma(1-\epsilon)} \theta(k_3^+ k_3^-) dk_3^+ dk_3^- \times \frac{2Q^2 (k_3^+ k_3^-)^{-\epsilon}}{(Qk_3^+ + p_1^2)(Qk_3^- + p_2^2)}, \tag{A1}$$

where $p_1^2 = Qk_1^+$, $p_2^2 = Qk_2^-$, and $p_3^2 = 0$. The JADE two-jet constraints become

$$\frac{M_{13}^2}{Q^2} = \frac{Qk_3^+ + p_1^2}{Q^2} < j, \qquad \frac{M_{23}^2}{Q^2} = \frac{Qk_3^- + p_2^2}{Q^2} < j, \qquad \frac{M_{12}^2}{Q^2} = 1 \tag{A2}$$

and integrating over the soft phase space gives

$$\frac{1}{\sigma_0}\sigma_{\mathrm{JADE}}^s = \frac{\alpha_s C_F}{2\pi}\left(\frac{1}{\epsilon}\left(4\ln j - 2\ln\frac{p_1^2}{Q^2} - 2\ln\frac{p_2^2}{Q^2}\right) + \left(\ln\frac{p_1^2}{Q^2} + \ln\frac{p_2^2}{Q^2}\right)^2 - 2\left(\ln\frac{p_1^2}{Q^2} + \ln\frac{p_2^2}{Q^2}\right)\ln\frac{\mu^2}{Q^2}\right) + \cdots \tag{A3}$$

where the ellipses denote finite constant terms.

Similarly, the SCET differential cross section for n-collinear gluon emission with off shellness is

$$\frac{1}{\sigma_0} d\sigma^n = \frac{\alpha_s C_F}{2\pi} \frac{\mu^{2\epsilon} e^{\epsilon\gamma_E}}{\Gamma(1-\epsilon)} dk_3^+ dp_3^- (p_3^- k_3^+)^{-\epsilon} \times \left(\frac{(1-\epsilon) p_3^- k_3^+}{(p_1^2 + Qk_3^+)^2} + \frac{2(Q - p_3^-)}{p_3^-(p_1^2 + Qk_3^+)}\right) \tag{A4}$$

and the corresponding JADE two-jet constraints are

$$\frac{M_{13}^2}{Q^2} = \frac{Qk_3^+ + p_1^2}{Q(Q - p_3^-)} < j, \qquad \frac{M_{23}^2}{Q^2} = \frac{Qp_3^- + p_2^2}{Q^2} < j, \qquad \frac{M_{12}^2}{Q^2} = \frac{Q(Q - p_3^-) + p_1^2 + p_2^2}{Q^2} < j. \tag{A5}$$

Note that the off shellnesses in M_{23}^2 and M_{12}^2 are suppressed with respect to the label momenta and thus can be dropped. Integrating Eq. (A4) over the phase space given by these constraints, we find

$$\frac{1}{\sigma_0}\tilde{\sigma}_{\mathrm{JADE}}^n = \frac{\alpha_s C_F}{2\pi}\left(-\frac{2}{\epsilon^2} + \frac{1}{\epsilon}\left(2\ln j + 2\ln\frac{p_1^2}{Q^2} - 2\ln\frac{\mu^2}{Q^2}\right) - \ln^2\frac{p_1^2}{Q^2} + 2\ln\frac{\mu^2}{Q^2}\ln\frac{p_1^2}{Q^2} + \frac{3}{2}\ln\frac{p_1^2}{Q^2}\right) + \ldots. \tag{A6}$$

The $p_3^- \to 0$ zero-bin for the n-collinear differential cross section is obtained from Eq. (A4) by taking the soft limit:

$$\frac{1}{\sigma_0} d\sigma^{n0} = \frac{\alpha_s C_F}{2\pi} \frac{\mu^{2\epsilon} e^{\epsilon\gamma_E}}{\Gamma(1-\epsilon)} dk_3^+ dp_3^- (p_3^- k_3^+)^{-\epsilon} \times \frac{2Q}{p_3^-(p_1^2 + Qk_3^+)}. \quad \text{(A7)}$$

The JADE constraints for this zero-bin are the same as the soft ones in Eq. (A2). Performing the phase space integration gives

$$\frac{1}{\sigma_0} \sigma^{n0}_{\text{JADE}} = \frac{\alpha_s C_F}{2\pi} \left(-\frac{2}{\epsilon^2} - \frac{2}{\epsilon} \ln \frac{\mu^2}{j^2 Q^2} \right) + \ldots. \quad \text{(A8)}$$

The zero-bin subtracted result, which is the difference between Eq. (A6) and (A8), is not particularly illuminating. It should be noted, however, that this zero-bin subtraction gets rid of the $1/\epsilon^2$ term, which is also absent in the contribution from soft gluon emission in Eq. (A3). Thus the total contribution from real gluon emission is free of such terms. The result for $\bar{n}$-collinear gluon emission will be the same as that for n-collinear gluon emission with $p_1^2 \to p_2^2$. Combining the real emission contributions to the JADE cross section gives

$$\begin{aligned} \frac{1}{\sigma_0} \sigma^R_{\text{JADE}} &= \frac{1}{\sigma_0} ((\tilde{\sigma}^n_{\text{JADE}} - \sigma^{n0}_{\text{JADE}}) + (\tilde{\sigma}^{\bar{n}}_{\text{JADE}} - \sigma^{\bar{n}0}_{\text{JADE}}) \\ &\quad + \sigma^s_{\text{JADE}}) \\ &= \frac{\alpha_s C_F}{2\pi} \left(2 \ln \frac{p_1^2}{Q^2} \ln \frac{p_2^2}{Q^2} + \frac{3}{2} \ln \frac{p_1^2}{Q^2} + \frac{3}{2} \ln \frac{p_2^2}{Q^2} \right) \\ &\quad + \ldots. \end{aligned} \quad \text{(A9)}$$

Notice that this result is free of ultraviolet divergences, and off shellness is regulating all of its infrared divergences. The collinear and the soft sectors are individually ultraviolet divergent, but these ultraviolet divergences arising from the phase space cancel completely with one another in the sum.

With off shellness, the virtual diagrams are no longer zero, and they have been previously calculated with off shellness, for example, in [19] for deep inelastic scattering and in [20] for e^+e^- annihilation. The zero-bin subtractions of the collinear virtual graphs also vanish with this regulator [18,23]. At the amplitude level, we sum up all the virtual vertex corrections and subtract half the wave function renormalization for each external (anti-)quark

$$\begin{aligned} I_V &= \frac{\alpha_s C_F}{4\pi} \left(\frac{2}{\epsilon^2} + \frac{3}{\epsilon} - \frac{2}{\epsilon} \ln \frac{-Q^2}{\mu^2} - 2 \ln \frac{p_1^2}{Q^2} \ln \frac{p_2^2}{Q^2} \right. \\ &\quad \left. - \frac{3}{2} \ln \frac{p_1^2}{Q^2} - \frac{3}{2} \ln \frac{p_2^2}{Q^2} \right) + \ldots. \end{aligned} \quad \text{(A10)}$$

The virtual graphs' contribution to the two-jet rate is $\sigma_V = 2\,\text{Re}(I_V)$. We can then see that the IR divergences from real gluon emission in Eq. (A9) will be completely cancelled by the virtual contributions, and the UV divergent terms in σ_V will be cancelled by the counterterm $|Z_2|^2$.

We can also focus on the soft sector to investigate its IR safety. The soft virtual vertex correction is given by [20]

$$I_V^s = \frac{\alpha_s C_F}{4\pi} \left(-\frac{2}{\epsilon^2} - \frac{2}{\epsilon} \ln \left(-\frac{\mu^2 Q^2}{p_1^2 p_2^2} \right) - \ln^2 \left(-\frac{\mu^2 Q^2}{p_1^2 p_2^2} \right) \right) + \ldots. \quad \text{(A11)}$$

The soft wave function renormalization graphs are zero, so in the soft sector, the soft virtual vertex correction and the soft gluon bremsstrahlung are the only two diagrams we need to add

$$\frac{1}{\sigma_0} (\sigma^s_{\text{JADE}} + \sigma^s_V) = \frac{\alpha_s C_F}{2\pi} \left(-\frac{2}{\epsilon^2} - \frac{4}{\epsilon} \ln \frac{\mu}{jQ} \right) + \ldots. \quad \text{(A12)}$$

This agrees with our pure dimensional regularization calculation in Eq. (12). This also shows that the rate in the soft sector is infrared finite. The collinear contribution is also IR safe because the sum of all sectors is free of infrared divergences.

$k_\perp$: The $k_\perp$ phase space regions shown in Table I are not affected by the introduction of the off shellnesses, with the only exception that the constraint

$$\min \left(\frac{k_3^+}{p_3^-}, \frac{k_3^+ p_3^-}{(Q - p_3^-)^2} \right) < y_c \quad \text{(A13)}$$

is slightly modified to

$$\min \left(\frac{Q - p_3^-}{p_3^-}, \frac{p_3^-}{Q - p_3^-} \right) \frac{Q^2 k_3^+ + p_3^- p_1^2}{Q^2 (Q - p_3^-)} < y_c. \quad \text{(A14)}$$

The calculation is otherwise straightforward.

[1] C. W. Bauer, S. Fleming, and M. E. Luke, Phys. Rev. D **63**, 014006 (2000).

[2] C. W. Bauer, S. Fleming, D. Pirjol, and I. W. Stewart, Phys. Rev. D **63**, 114020 (2001).

[3] C. W. Bauer and I. W. Stewart, Phys. Lett. B **516**, 134 (2001).

[4] C. W. Bauer, D. Pirjol, and I. W. Stewart, Phys. Rev. D **65**, 054022 (2002).

[5] C. W. Bauer, S. Fleming, D. Pirjol, I. Z. Rothstein, and I. W. Stewart, Phys. Rev. D **66**, 014017 (2002).

[6] J. C. Collins, D. E. Soper, and G. Sterman, Adv. Ser. Dir. High Energy Phys. **5**, 1 (1988).

[7] G. Sterman, arXiv:hep-ph/9606312.
[8] C. W. Bauer, A. V. Manohar, and M. B. Wise, Phys. Rev. Lett. **91**, 122001 (2003).
[9] C. W. Bauer, C. Lee, A. V. Manohar, and M. B. Wise, Phys. Rev. D **70**, 034014 (2004).
[10] C. W. Bauer, S. P. Fleming, C. Lee, and G. Sterman, Phys. Rev. D **78**, 034027 (2008).
[11] A. Hornig, C. Lee, and G. Ovanesyan, J. High Energy Phys. 05 (2009) 122; Phys. Lett. B **677**, 272 (2009).
[12] S. Fleming, A. H. Hoang, S. Mantry, and I. W. Stewart, Phys. Rev. D **77**, 074010 (2008).
[13] C. W. Bauer, A. Hornig, and F. J. Tackmann, Phys. Rev. D **79**, 114013 (2009).
[14] G. Sterman and S. Weinberg, Phys. Rev. Lett. **39**, 1436 (1977).
[15] M. Trott, Phys. Rev. D **75**, 054011 (2007).
[16] S. Bethke *et al.* (JADE Collaboration), Phys. Lett. B **213**, 235 (1988).
[17] S. Catani, Y. L. Dokshitzer, M. Olsson, G. Turnock, and B. R. Webber, Phys. Lett. B **269**, 432 (1991).
[18] A. V. Manohar and I. W. Stewart, Phys. Rev. D **76**, 074002 (2007).
[19] A. V. Manohar, Phys. Rev. D **68**, 114019 (2003).
[20] C. W. Bauer and M. D. Schwartz, Phys. Rev. D **76**, 074004 (2007).
[21] A. Idilbi and T. Mehen, Phys. Rev. D **75**, 114017 (2007).
[22] A. Idilbi and T. Mehen, Phys. Rev. D **76**, 094015 (2007).
[23] J.-Y. Chiu, A. Fuhrer, A. H. Hoang, R. Kelley, and A. V. Manohar, Phys. Rev. D **79**, 053007 (2009).
[24] G. Kramer and B. Lampe, Z. Phys. C **34**, 497 (1987); **42**, 504(E) (1989).
[25] N. Brown and W. J. Stirling, Z. Phys. C **53**, 629 (1992).
[26] N. Brown and W. J. Stirling, Phys. Lett. B **252**, 657 (1990).
[27] S. Mukhi and G. Sterman, Nucl. Phys. **B206**, 221 (1982).
[28] J. Y. Chiu, A. Fuhrer, R. Kelley, and A. V. Manohar, Phys. Rev. D **80**, 094013 (2009).